

Article

# Surface Discharge Analysis of High Voltage Glass Insulators Using Ultraviolet Pulse Voltage

Saiful Mohammad Iezham Suhaimi <sup>1</sup>, Nouruddeen Bashir <sup>2</sup> , Nor Asiah Muhamad <sup>3,\*</sup> ,  
Nurun Najah Abdul Rahim <sup>3</sup>, Noor Azlinda Ahmad <sup>4</sup> and Mohd Nazri Abdul Rahman <sup>5</sup> 

<sup>1</sup> Tenaga Nasional Berhad, Tumpat, Kelantan 16250, Malaysia; saifuliezham@gmail.com

<sup>2</sup> Power Equipment & Electrical Machinery Development Institute (PEEMADI),  
National Agency for Science and Engineering Infrastructure (NASENI), P.M.B 1029 Okene,  
Kogi State, Nigeria; nouruddeen@gmail.com or nour@utm.my

<sup>3</sup> School of Electrical and Electronic Engineering, Universiti Sains Malaysia (USM), Nibong Tebal 14300,  
Malaysia; nurunnajah3194@gmail.com

<sup>4</sup> Institute of High Voltage and High Current (IVAT), Universiti Teknologi Malaysia, Skudai, Johor 81310,  
Malaysia; noorazlinda@utm.my

<sup>5</sup> Faculty of Education, University of Malaya, Kuala Lumpur 50603, Malaysia; mohdnazri\_ar@um.edu.my

\* Correspondence: norasiah.m@usm.my; Tel.: +604-599-5726

Received: 14 December 2018; Accepted: 7 January 2019; Published: 9 January 2019



**Abstract:** Surface discharges are precursors to flashover. To pre-empt the occurrence of flashover incidents, utility companies need to regularly monitor the condition of line insulators. Recent studies have shown that monitoring of UV signals emitted by surface discharges of insulators is a promising technique. In this work, the UV signals' time and frequency components of a set of contaminated and field-aged insulator under varying contamination levels and degrees of ageing were studied. Experimental result shows that a strong correlation exists between the discharge intensity levels under varying contamination levels and degree of ageing. As the contamination level increases, the discharge level of the insulator samples also intensifies, resulting in the increase of total harmonic distortion and fundamental frequencies. Total harmonic distortion and fundamental frequencies of the UV signals were employed to develop a technique based on artificial neural networks (ANNs) to classify the flashover prediction based on the discharge intensity levels of the insulator samples. The results of the ANN simulation showed 87% accuracy in the performance index. This study illustrates that the UV pulse detection method is a potential tool to monitor insulator surface conditions during service.

**Keywords:** contamination flashover; ultraviolet; glass insulator; total harmonic distortion; artificial neural network; surface discharges

## 1. Introduction

Transmission line insulators are susceptible to contamination flashover, and thus are a source of power system failure. The energy transferred through the transmission line is usually at its highest level to avoid losses since it is transferred over a long distance. Thus, insulators used on transmission lines need to have adequate insulation for the particular voltage level they are operating. Although they have been designed for that voltage level, environmental factors need to be considered as they affect the insulators' performance [1]. The environment is one of the main causes of insulator flashover and breakdown in power systems. Aerosols and pollutants deposited on the surface of the insulators cause reduction in insulator surface resistance, thereby leading to the flow of leakage current (LC) [2]. This subsequently leads to the formation of surface discharges on the surface of the insulators.

Since the environment in which the insulators operate cannot be controlled, electricity supply companies carry out maintenance services to prevent or reduce surface discharges from developing into a flashover. The maintenance methods usually practiced by the utility companies are either breakdown maintenance or periodic maintenance. However, nowadays researchers are studying and developing methods to predict the insulators' surface conditions during their operation to prevent flashover occurrences. Such a kind of maintenance method is called predictive maintenance. In such cases, the surface discharges that develop on the surface of insulators which are precursors to flashover incidences can be monitored.

Insulator surface discharge needs to be monitored closely over time since the pollution around the insulators are unpredictable. The various methods that have been used to detect surface discharges include infrared method, ultrasonic method, acoustics method, leakage current method, and ultraviolet method, with each method having its pros and cons [3–5]. By detecting the discharge that happens on the surface of the insulators, the flashover can also be predicted and thus minimize power system failure. Table 1 summarizes the pros and cons of some of the detection methods used.

**Table 1.** Pros and cons of various detection methods.

Detection Method	Pros	Cons
Leakage current	<ul style="list-style-type: none"> <li>• Simple</li> <li>• Cheap</li> </ul>	<ul style="list-style-type: none"> <li>• Direct contact measurement</li> </ul>
Acoustic	<ul style="list-style-type: none"> <li>• Immune to electromagnetic interference</li> </ul>	<ul style="list-style-type: none"> <li>• Used for partial discharge detection</li> </ul>
Ultrasonic	<ul style="list-style-type: none"> <li>• Easily locates discharge</li> <li>• Non-contact measurement</li> </ul>	<ul style="list-style-type: none"> <li>• Poor sensitivity</li> <li>• Sound attenuation</li> </ul>
Infrared	<ul style="list-style-type: none"> <li>• Temperature detection</li> <li>• Non-contact measurement</li> </ul>	<ul style="list-style-type: none"> <li>• Detection accuracy affected by weather (hot and sunny days)</li> </ul>
Ultraviolet imaging	<ul style="list-style-type: none"> <li>• High accuracy</li> <li>• Non-contact measurement</li> </ul>	<ul style="list-style-type: none"> <li>• Expensive</li> </ul>

Studies have shown that surface discharges on the surface of insulators emit UV radiation [6]. Ultraviolet radiation can be detected from many sources, such as sunlight, electric discharge, and special light (e.g., mercury–vapor lamps, back light) [7]. These UV radiations have different wavelengths. The UV radiation from electrical discharges such as corona have a waveband of 280–400 nm, while few others range from 160 nm to 180 nm [8]. These wavebands are also known as the solar blind region.

Many researchers have studied the UV radiation emitted from electrical discharge using the UV image method [9–13]. This method is reliable since it can detect and pinpoint the discharge location, though it is very expensive when used in the field. However, other inexpensive UV signal detection methods have been proposed. One of these methods is the UV pulse method. This method involves the detection and measurement of UV pulses due to UV radiation emitted by the insulator surface discharges. This method has been shown to be promising.

The paper presents laboratory studies on the detection and measurement of UV emission due to discharge activities on the surfaces of contaminated and field-aged ceramic insulators using the UV pulse voltage method. Various surface discharge intensities were generated under various contamination levels and degree of ageing. The detected UV pulse signals' time and frequency components were studied. Furthermore, pattern recognition techniques using an artificial neural

networks (ANN) was employed and applied to the positively correlated parameters to predict the imminence and severity of contamination flashover incidence.

## 2. Materials and Methods

### 2.1. Insulators Samples

Glass (ceramic) insulator samples were used and grouped into Group A, Group B, and Group C. The insulators were obtained from the 132-kV transmission line network of the Malaysian national power company, Tenaga Nasional Berhad. The insulators sampled were standard insulators having a leakage distance of 290 mm. Table 2 shows the description of the insulators sampled, respectively.

**Table 2.** Insulators sampled (description).

Insulator Samples (Group)	Service History	Number of Samples	State/Degree of Ageing	Picture of Sample
A	Less than 10 years	2	Good condition	
B	Between 10 and 20 years	2	Mild corrosion at cap	
C	Greater than 20 years	2	Discoloration of glass dielectric, severely corroded cap and pin	

### 2.2. Experimental Setup

#### 2.2.1. Test Chamber

The test chamber was designed and fabricated for the purpose of this study. Figure 1 shows the experimental setup of this study. A 100-kV step-up transformer was used to inject high voltage to the insulator sample. The high-voltage supply from the transformer was controlled using a voltage regulator. The insulator sample was housed in the chamber made up of acrylic glass. The dimension of the chamber as  $80 \times 80 \times 80$  cm. In this study, applied voltages ranging from 25 kV to 65 kV were used depending on the desired discharge intensity level to be generated.

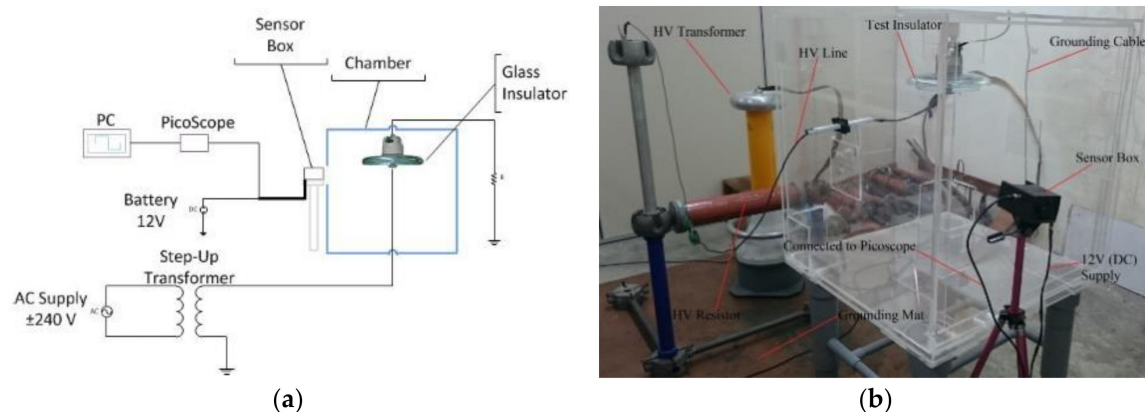


**Figure 1.** Experimental setup: (a) schematic diagram and (b) pictorial view.

### 2.2.2. Detection and Measurement of UV Signal

The UV radiation emitted during discharge activities was detected using a UV pulse sensor which was placed outside of the chamber. The sensor was powered by a 12 V DC battery. The output of the sensor was connected to a computer via an analog-to-digital converter (PicoScope 5244B, 2 Channel, 200 MHz, 500 MSPS, 512 Mpts, 5.8 ns). The UV sensor (UV TRON R2868, manufactured by Hamamatsu Company, Shizuko Japan) was used to detect the UV signals during discharges. The UV sensor can detect UV signals with wavelengths between 160 nm and 280 nm. The sensor comes along with its driving circuit, UVTRON Driving Circuit C3704. The driving circuit activates the sensor in the event of a discharge. Figure 2 shows the response range of the UV sensor. The UV sensor can detect UV radiation 5 m from the source. Detailed specification of the sensor has been described in Reference [14]. In this study, the UV sensor and driver circuitry were housed in a box and placed just outside the insulator test chamber. PicoScope software installed in the computer was used for measuring and recording the UV pulse signals data. The PicoScope software acted as a digital oscilloscope. The signal data were saved in PicoScope files before being transferred into Microsoft Excel and MATLAB for further analysis. MATLAB was used to remove the noise in the signals to make it easier for pattern identification, and also to find the harmonic distortion of the signals.

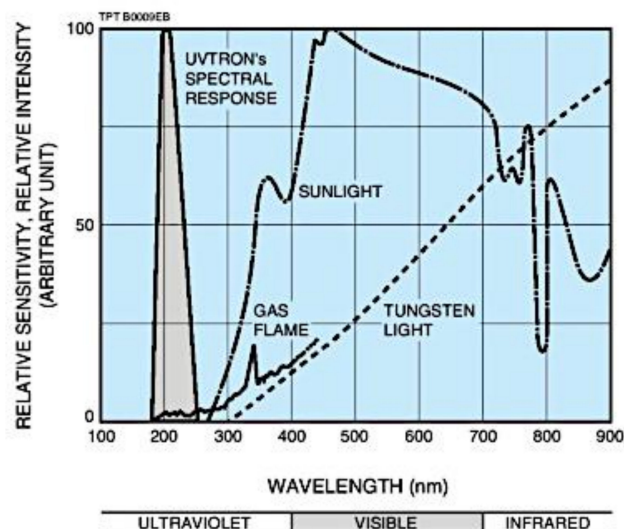


Figure 2. Response range of the UV sensor [14].

### 2.3. Artificial Contamination

In this study, the insulator samples were artificially contaminated with salt according to IEC 60507 [15]. The insulators were contaminated with 3 different salinity levels. To contaminate an insulator sample, a known amount of salt is dissolved in a liter of water and then sprayed on the insulator surface using a spray bottle. The equivalent salt deposit density (ESDD) of the salinity levels were computed using IEC 60507. The IEC 60815 [16] was used to determine the contamination severity of the 3 salinity levels used based on the computed ESDD. Table 3 shows the salt amount and the corresponding ESDD and contamination level.

Table 3. Insulator samples' artificial contamination.

Salt (g/L)	ESDD (mg/cm <sup>2</sup> )	Contamination Level
0	N/A	N/A
5	0.06	Light
30	0.21	Medium
120	0.47	High

ESDD: Equivalent Salt Deposit Density.

#### 2.4. Insulator Surface Discharge

Discharges are local breakdowns due to increased electrical stress. In order to generate the discharges of various intensities on the surface of the insulator samples, the applied voltage was varied. Various discharge intensities were generated to closely mimic service condition as well as processes that lead to flashover of insulator during service. Voltage was applied starting from zero and increased continuously until the required discharge intensity level was reached. Once the required discharge intensity level was reached, the applied voltage, UV signal voltages, and waveforms were recorded. Table 4 depicts the discharge intensities produced in this study.

**Table 4.** Classification of insulator surface discharge intensity levels.

Insulator Condition	Discharge Intensity Level	Description
Dry	Hissing	Hissing without any visible discharge
	Discharge at pin	Hissing sound plus spot discharge at both the pin and cap of insulator samples
	Discharge at cap of the insulator	Louder hissing noise, discharges at both pin and cap of the insulator samples
	Severe discharge	Very loud hissing noise, intense sparing discharge on the pin and cap of the insulator (just prior to flashover)
Wet	Hissing	Hissing sound without visible discharge
	Spot discharge	Spot discharge appear on insulator surfaces (depending on contamination level, this condition takes place sometimes when hissing sound is heard)
	Continuous discharge	Continuous discharges on insulator surfaces
	Severe discharge	Severe continuous discharge on entire insulator surfaces

#### 2.5. Data Analysis

Fast Fourier Transform (FFT) was used in this study to compute the total harmonic distortion (THD) values of the detected UV signals saved. The FFT analysis was done using MATLAB software using Simulink block diagram tools. The saved UV signal data in PicoScope software were transferred to Microsoft Excel then transferred to MATLAB. Figure 3 shows the block diagram of the FFT analysis to determine the THD and frequency component of the signals. The THD was used in this work to study the distorted UV signals caused as a result of the presence of discharges. Total harmonic distortion is the ratio between the root-mean-square (RMS) values of harmonics and the RMS value of the fundamental.

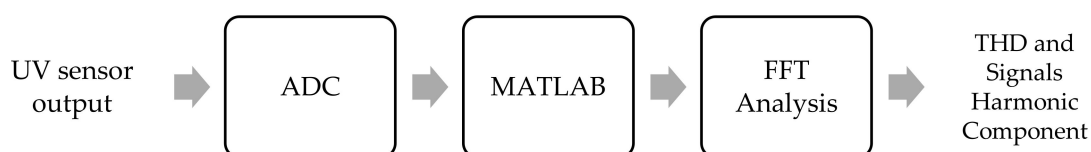


**Figure 3.** Schematic diagrams for Fast Fourier Transform (FFT) analysis involving ultra violet (UV) sensor, AC to DC converter (ADC), MATLAB Software, Fast Fourier Transformer (FFT) analysis and lastly the total harmonic distortion (THD) analysis.

#### 2.6. Flashover

In this study, pattern recognition using ANN was used to identify and classify discharge intensity levels under various insulator surface conditions vis-à-vis contamination level, contamination state and degree of ageing. The pattern recognition results were used to predict the imminence of contamination flashover incidence. Figure 4 shows the pattern recognition process using ANN.

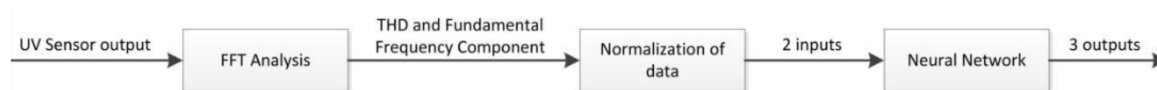


**Figure 4.** Process of pattern recognition using ANN.

Based on the intensity levels of the surface discharge intensifies both under dry and wet conditions, this study developed contamination flashover severity level based on the insulator surface condition and discharge intensity levels as shown in Table 5.

**Table 5.** Flashover indication level.

Surface Condition	Discharge Intensity Levels	Flashover Indication
Dry	Hissing	Warning
	Discharge at Pin	Danger (Dry)
	Discharge at Cap Severe	
Wet	Hissing	Warning
	Spot Discharge	Danger (Wet)
	Continuous Discharge Severe	

### 2.6.1. Normalization of ANN Input Data Variables

The UV pulse data (frequency components) were normalized to be in range of 0 to 1 using Equation (1) [17] below before using them as inputs to the ANN. This equation is a standard mathematical equation used to normalize sets of data. Normalization is a technique of preprocessing data to ensure a uniform statistical distribution of each input value. If the input and the output variables are not of the same order of magnitude, some variables may appear to have more significance than the actual data. The ANN input takes data of the range 0 to 1; the experimental data are either within 0 to 1, or outside this range. So, the data has to be normalized to be within the 0 to 1 range [17].

$$V = V_{min} + (V_{max} - V_{min}) \left[ \frac{D - D_{min}}{D_{max} - D_{min}} \right] \quad (1)$$

where  $V_{max}$  and  $V_{min}$  are the input range of the ANN.  $D$  is the input value of the data while  $D_{min}$  and  $D_{max}$  are the minimum and maximum values of the input data.

### 2.6.2. Artificial Neural Network

The ANN was designed using the MATLAB Neural Network Toolbox. Based on the relationship between the discharge intensity levels and UV signals' THD and fundamental frequencies, the input of the ANN were harmonic components of the UV signals. In this study, the ANN designed had three layers. The input layer (with two inputs), two hidden layers with nine and eleven neurons, respectively, and the output layer with three outputs. Figure 5 depicts the ANN architecture. The THD and fundamental frequency components of the UV signal were used as the input of the ANN.

The output values of the ANN correspond to the three categorized flashover indication levels. Table 6 shows the relationship between the ANN output neuron value and the flashover indication levels. In this study, 98 sets of experimental data were used. In the training phase, 68 data sets were used to train the neural network. The data comprised of 28 different sets of data to train the ANN on "warning" flashover level, while 20 data sets each were used to train the ANN for "danger (dry condition)" and "danger (wet condition)", respectively. The remaining 30 sets of data (which were not used for the training) were used to test the ANN. The data used for the ANN training and testing were the frequency components of various discharge intensity levels under different insulator surface conditions as summarized in Table 5.

**Table 6.** Relationship between the output values of artificial neural network (ANN) and flashover indication.

Output Neuron Value 1 2 3	Flashover Indication
1 0 0	Warning
0 1 0	Danger (dry condition)
0 0 1	Danger (wet condition)

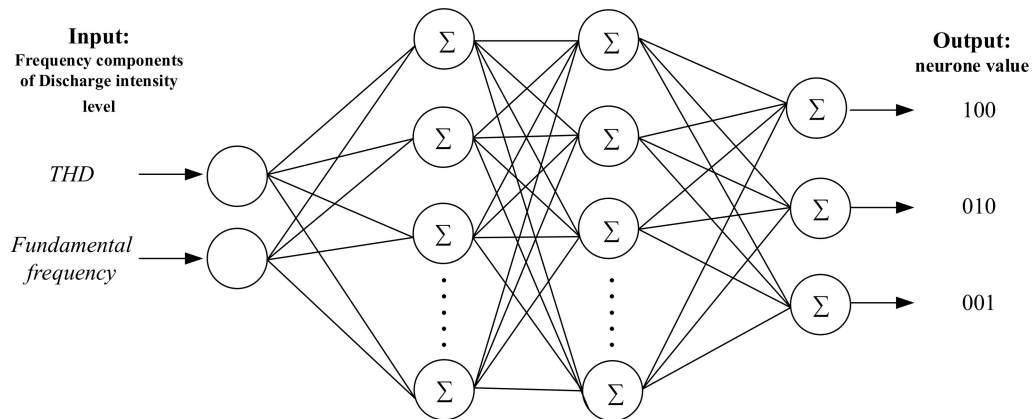


**Figure 5.** ANN architecture.

### 3. Results and Discussions

#### 3.1. Flashover

The UV sensor connected to the PicoScope produces sinusoidal waveform at the output of circuit driver in the absence of any UV signal detected from surface discharges. A low voltage not high enough to produce a discharge was applied to the insulator sample. Figure 6 shows the sensor output in the absence of any detected UV signal.

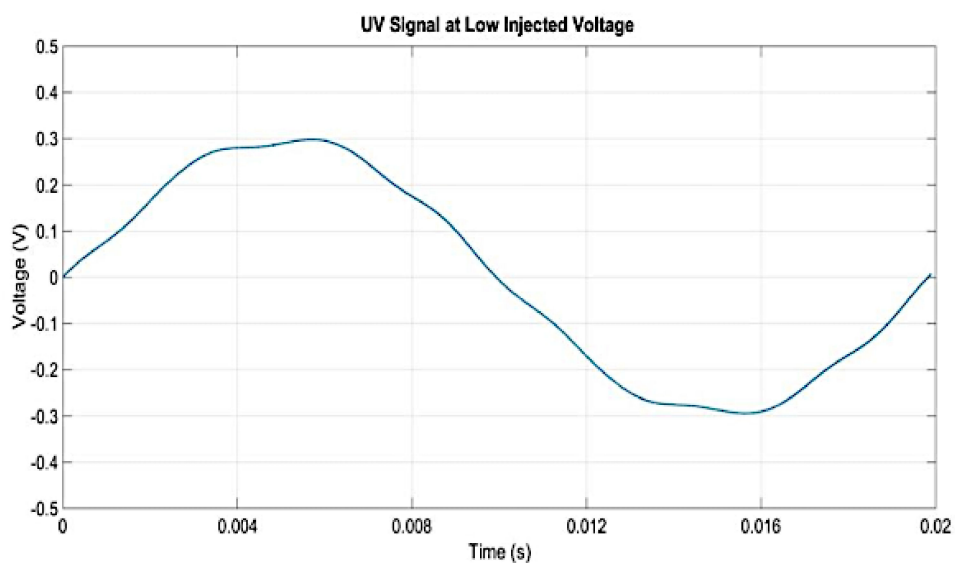


**Figure 6.** Signals detected at low injected voltage.

From Figure 6 it can be seen that the waveform of a frequency of 50 Hz (having a period of 0.02 s) is the same as the injected voltage of the insulator. Each frame of the PicoScope is taken in 100 ms so that analyses will be easier. MATLAB was used to re-plot the signals' waveform.

### 3.2. UV Due to the Presence of Surface Discharge

This section presents and discusses the results of the measured and recorded UV signals detected during discharge activities on the surfaces of the insulator samples under the varying degrees of contamination and ageing for dry and wet insulator surfaces.

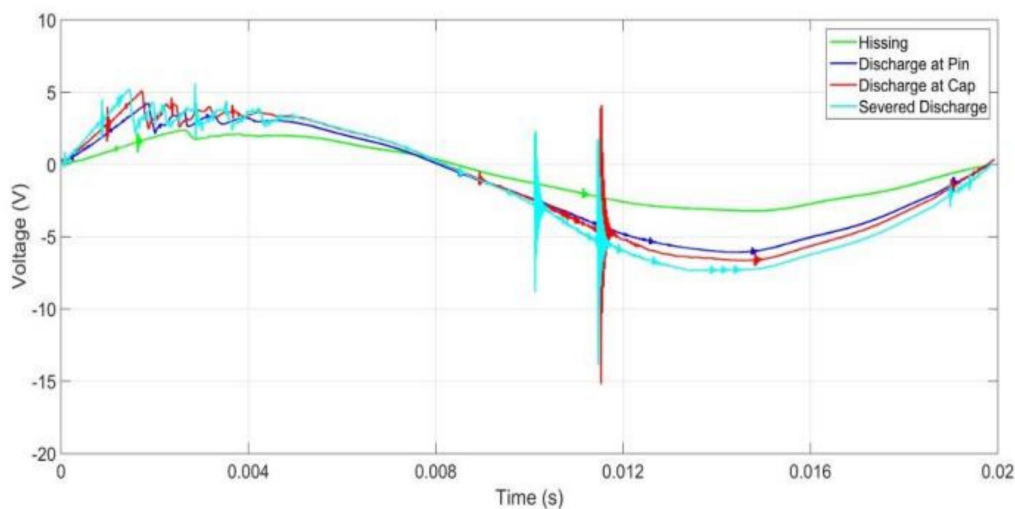
#### 3.2.1. Clean Insulator Samples

Contamination on the surface of insulators could be washed away because of rain or snow rendering an aged or unaged insulator surface free from contamination. Furthermore, the uncontaminated insulator may experience wetness on its surface due to dew, drizzles, etc., or become dry in the presence of sun, etc. The cleaning method for the insulator was done according to the IEC 60305 standard [18]. These service conditions were mimicked according to IEC 60507 [15] in the laboratory and UV signals due to the presence of discharges were investigated.

#### Dry Conditions

Under dry conditions, the insulator samples were cleaned from any conductive materials on the surfaces. The results for dry insulators conditions are shown in Figure 7. From the figure, it can be seen that the magnitude of the UV signal waveforms increased with increasing discharge intensities for all the insulator sample groups. Hissing condition had the lowest magnitude while severe discharge had the highest. In addition, the magnitude of the UV signals also increased with the degree of ageing. Group C insulators, which were severely corroded, had the highest voltage waveform magnitude, while Group A, which were in good condition, had the lowest. Group C insulator samples also had higher pulses compared to Group B and Group A samples.

A trend could also be observed concerning the number of disturbances due to the presence of discharges in the first and second half cycles of the signals. In the first half cycle, hissing had the least disturbances, with the number of disturbances increasing with increasing discharge intensities. This was also observed in the second half cycle albeit with higher disturbances compared to the first half cycle. Additionally, the disturbances in the second half cycles for lower discharge intensities were minimal.



(a)

Figure 7. Cont.

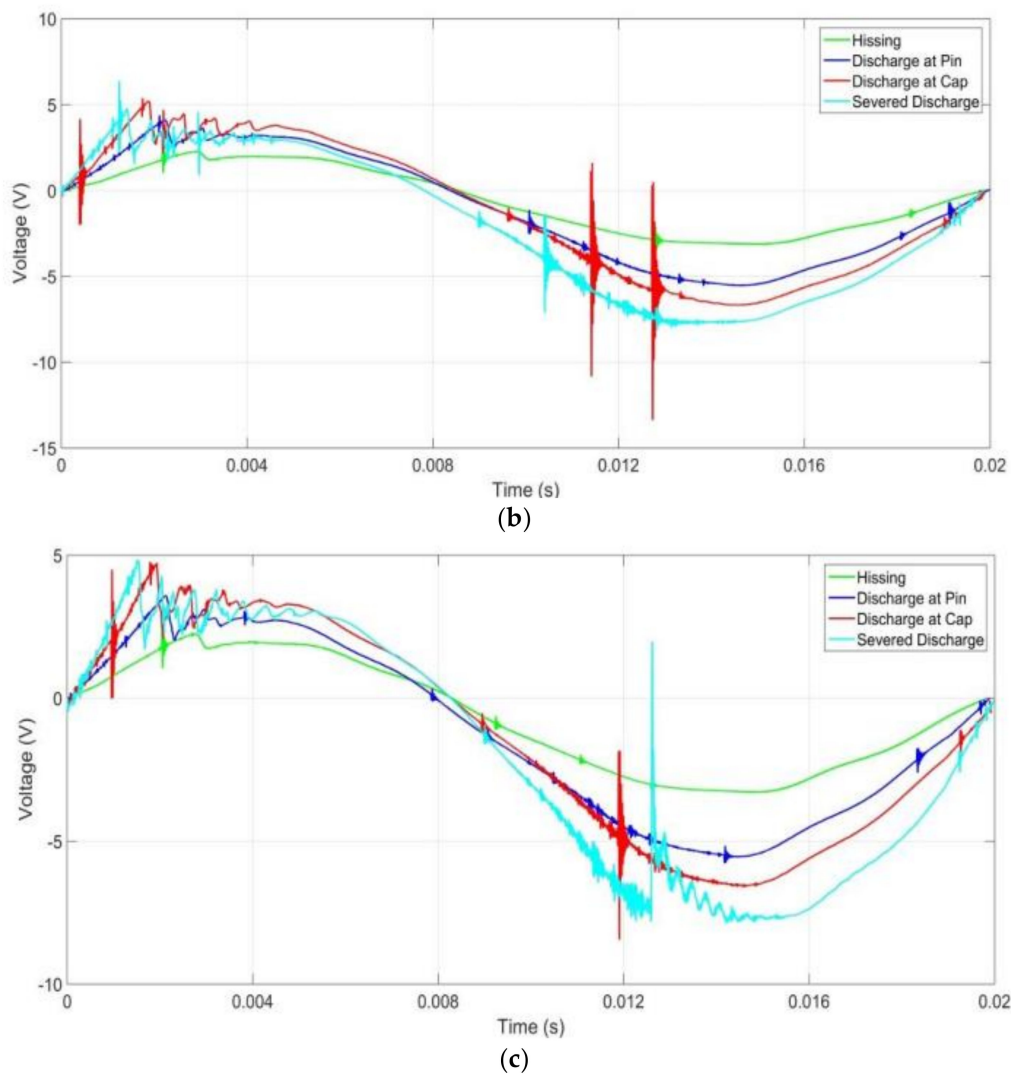


**Figure 7.** UV signals for insulator samples with dry surface conditions and without contaminations: (a) Group A; (b) Group B; (c) Group C.

Table 7 presents the injected voltages (required to create the necessary stress on the surface of the insulators) and the average peak-to-peak value of the UV signals. It can be seen that there is a correlation between the UV signal peak-to-peak amplitude (detected by the UV sensor) and the discharge intensity levels. As the discharge intensity levels of the insulators increase, the UV signals detected due to the UV radiated from the discharges increased as well.

**Table 7.** Injected voltage and average peak-to-peak voltages of the UV signals for dry insulators conditions without contamination.

Insulator Samples (Group)	Voltages		
	Discharge Intensity Level	Range Injected Voltage, $V_i$ (kV)	Average Peak to Peak Voltage, $V_{p-p}$ (V)
A	Hissing	27–35	5.6
	Discharge at Pin	40–50	10.3
	Discharge at Cap	54–56	11.6
	Severe	60–63	12.5
B	Hissing	27–33	5.6
	Discharge at Pin	40–47	9.1
	Discharge at Cap	52–55	11.2
	Severe	59–63	12.5
C	Hissing	27–34	5.4
	Discharge at Pin	42–48	9.6
	Discharge at Cap	51–54	11.8
	Severe	59–63	12.3

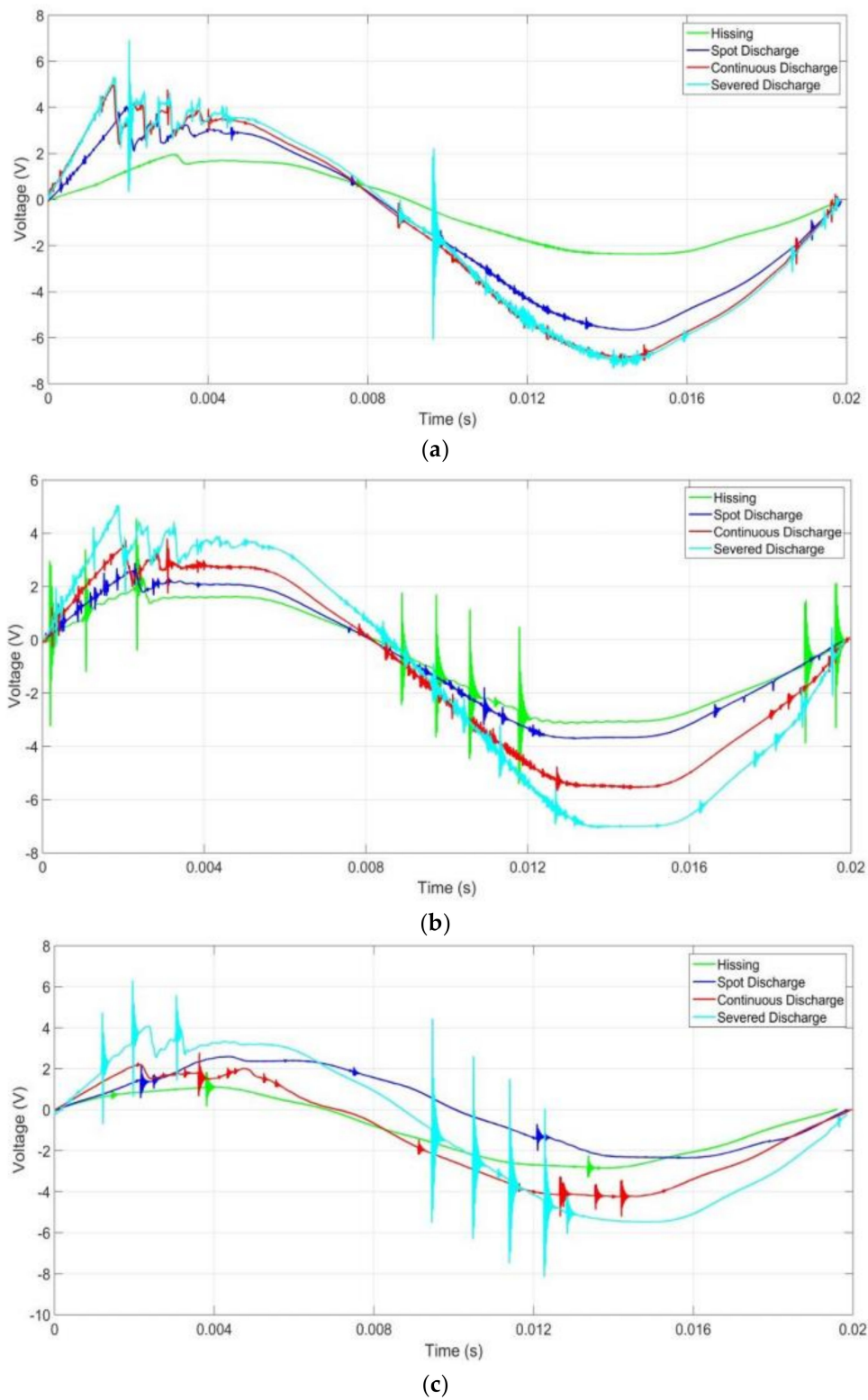
### Wet Conditions

In the case of wet conditions, clean water was sprayed on the insulator surface (without any contamination). As earlier mentioned, this condition represents clean insulators in the field having wet surface due to rain, drizzle or humidity (in the night). The intensity of the discharge during the wet conditions is different from dry conditions. The results of detected UV signals for wet conditions are shown in Figure 8.

When the surfaces of the insulator samples are wet, they will possess lower resistances compared to the dry-surfaced insulators, thus higher magnitude LC will flow. Similar to the UV signal waveforms presented under dry conditions (Figure 7), it can also be seen that a correlation exists between the UV signal magnitudes and discharge intensities. Likewise, the number of disturbances in each half cycle. However, the disturbances in the case of wet conditions are higher/severer than those under the dry conditions. In addition, the UV signal waveforms of aged insulators (Group B and C) had more disturbances than the unaged insulators (Group A).

Table 8 shows the values of injected voltages and UV signals peak-to-peak values under wet conditions. It can be seen from the table that the injected voltage needed to produce the discharge intensities were lower compared to dry conditions. This was due to the low surface resistance the insulator samples possessed as a result of wetting (moisture). In addition, there was not a marked difference in the average peak-to-peak values of the UV signals. However as earlier mentioned, the disturbances due to the discharge activities (which reflected on the waveforms) were higher when compared to dry condition.

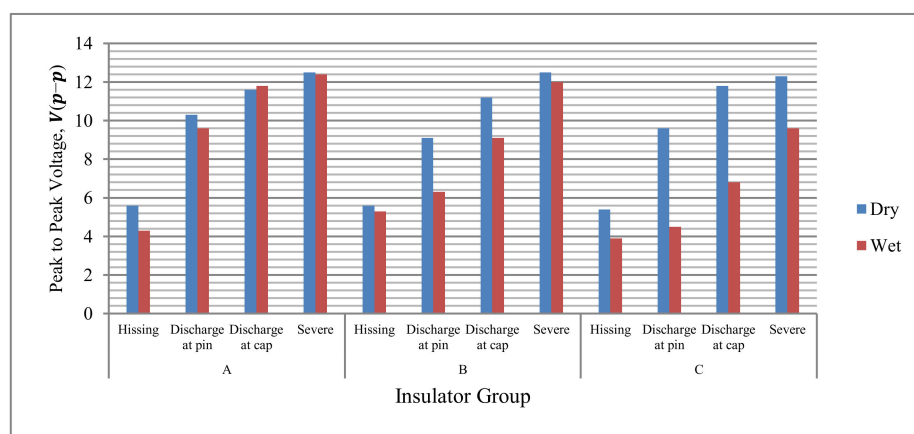
Figure 9 presents a comparison between the UV signal peak-to-peak voltages of the insulator samples under dry and wet condition. The increasing trend can be seen from hissing to severe discharge intensity level for all groups of insulators. However, the voltage amplitudes of the most aged insulators (Group C) under wet conditions was the lowest. This is because this group of insulators were the most severely corroded, thus when wet, they will possess the lowest surface resistance; this implies that lower injected voltage was required to generate surface discharges with high intensity.



**Figure 8.** UV signals for insulator samples with wet insulator conditions without contamination: (a) Group A; (b) Group B; (c) Group C.

**Table 8.** Injected voltage and average peak-to-peak voltages of the UV signals for wet insulators conditions without contamination.

Samples Group	Voltages		
	Discharge Intensity Level	Range Injected Voltage, $V_i$ (kV)	Average Peak to Peak Voltage, $V_{p-p}$ (V)
A	Hissing	15–18	4.3
	Spot Discharge	23–30	9.6
	Continuous Discharge	30–46	11.8
	Severe	50–53	12.4
B	Hissing	15–20	5.3
	Spot Discharge	22–30	6.3
	Continuous Discharge	31–44	9.1
	Severe	50–54	12.0
C	Hissing	14–20	3.9
	Spot Discharge	20–21	4.5
	Continuous Discharge	25–29	6.8
	Severe	38–51	9.6

**Figure 9.** Peak-to-peak voltage for dry and wet conditions without contamination.

### 3.2.2. Contaminated Insulator Samples

In this section, the aged insulator samples were contaminated with different levels of contamination (light, medium, and high).

#### Dry Condition

Contaminated insulators with dry conditions in service often happen when the insulators have been polluted with industrial pollutions, smoke from vehicles, etc., or coastal pollution such as salt sprays from the sea, which then get dried up under hot and sunny days. In this study, to replicate this type of field contamination in the laboratory, the surfaces of the insulator samples were sprayed with saline solution and then dried out under the sun for 6 h [13]. Figure 10 shows the UV signal waveforms of lightly contaminated insulator samples under dry conditions.

From Figure 10, it can be seen that the UV signal waveforms vis-à-vis magnitude and disturbances are similar to clean insulator samples under dry conditions, however, with more disturbances observed. Appendix A shows the UV signals for insulator samples with medium and heavy contamination. Tables 9–11 show the injected voltages and average peak-to-peak voltage of the UV signal waveforms for the contaminated insulator samples under dry conditions for light, medium, and heavy contamination levels, respectively.

From the UV signal waveforms, injected voltages, and peak-to-peak voltages results, it can be seen that the UV signals magnitude were mostly increasing as the intensity of the discharge increased.

Although some of the signals' peak-to-peak voltages were decreasing from discharge at cap to severe discharges. In addition, the disturbances were higher when compared to dry condition without contamination. The disturbances in the first half cycles of the UV signals were also having increasing trends as the discharge intensities increased. Figure 11 shows the graph of insulator samples' UV signal peak-to-peak voltages for dry condition at each level of contamination.

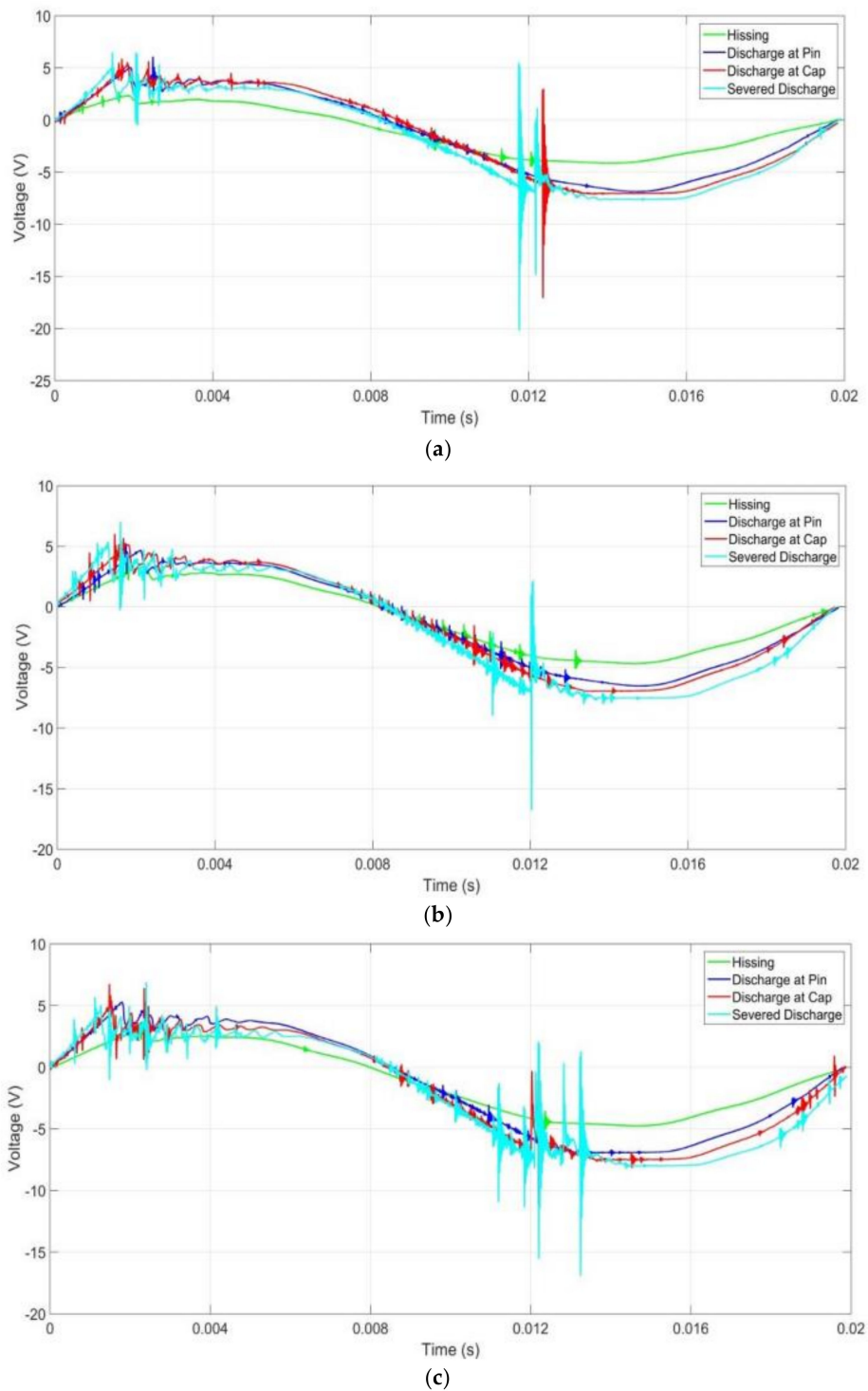


**Figure 10.** UV signals for insulator samples under dry conditions with light contamination level: (a) Group A; (b) Group B; (c) Group C.

**Table 9.** Injected voltage and average peak-to-peak voltages of the UV signals for dry insulators conditions with light contamination level.

Sample	Group A		Group B		Group C	
	Range Injected Voltage, $V_i$ (kV)	Average Peak-to-Peak Voltage, $V_{p-p}$ (V)	Range Injected Voltage, $V_i$ (kV)	Average Peak-to-Peak Voltage, $V_{p-p}$ (V)	Range Injected Voltage, $V_i$ (kV)	Average Peak-to-Peak Voltage, $V_{p-p}$ (V)
Hissing	20–32	6.4	19–32	8.0	18–28	7.7
Discharge at pin	42–50	11.8	41–49	11.2	40–47	12.2
Discharge at cap	50–54	12.4	49–54	12.1	50–54	13.3
Severe	60–63	12.6	60–63	12.9	59–62	13.0

**Table 10.** Injected voltage and average peak-to-peak voltages of the UV signals for dry insulators conditions with medium contamination level.

Sample	Group A		Group B		Group C	
	Range Injected Voltage, $V_i$ (kV)	Average Peak-to-Peak Voltage, $V_{p-p}$ (V)	Range Injected Voltage, $V_i$ (kV)	Average Peak-to-Peak Voltage, $V_{p-p}$ (V)	Range Injected Voltage, $V_i$ (kV)	Average Peak-to-Peak Voltage, $V_{p-p}$ (V)
Hissing	20–32	6.3	19–32	5.7	19–31	8.6
Discharge at pin	40–50	11.0	40–46	11.5	40–47	12.1
Discharge at cap	50–54	12.1	48–51	11.8	51–55	12.2
Severe	60–63	12.5	58–62	12.6	58–62	12.7

**Table 11.** Injected voltage and average peak-to-peak voltages of the UV signals for dry insulators conditions with heavy contamination level.

Sample	Group A		Group B		Group C	
	Range Injected Voltage, $V_i$ (kV)	Average Peak-to-Peak Voltage, $V_{p-p}$ (V)	Range Injected Voltage, $V_i$ (kV)	Average Peak-to-Peak Voltage, $V_{p-p}$ (V)	Range Injected Voltage, $V_i$ (kV)	Average Peak-to-Peak Voltage, $V_{p-p}$ (V)
Hissing	20–31	6.5	19–32	8.2	19–34	6.8
Discharge at pin	35–48	11.9	37–43	11.9	32–44	12.2
Discharge at cap	44–49	12.2	47–51	12.4	46–52	12.6
Severe	56–59	12.2	56–60	12.2	56–60	13.0

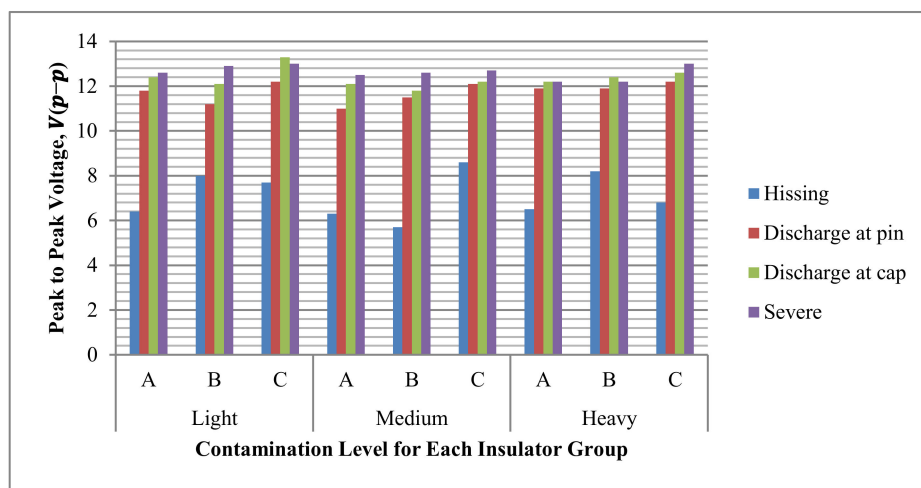


**Figure 11.** Average peak-to-peak voltage for all insulator sample groups for all contamination levels under dry condition.

**Wet Conditions**

Under wet conditions, the insulator surfaces were sprayed with salt contaminants of different contamination levels and experiment were conducted while their surfaces were still wet. Figure 12 shows the results of the UV signals for light contamination under wet conditions. The UV signal waveforms for medium and heavy contamination levels are shown in Appendix B. It can be seen from

the waveforms that the disturbances on the UV signal waveforms were very high, much higher than wet conditions for clean insulators. In addition, the waveforms were highly distorted especially the aged insulator samples (Group B and C). The corrosion on the insulator surfaces provided a conductive path which along with the moist surface made their surface resistances to be drastically reduced, thus leading to severe discharge activities even at lower electrical stresses.

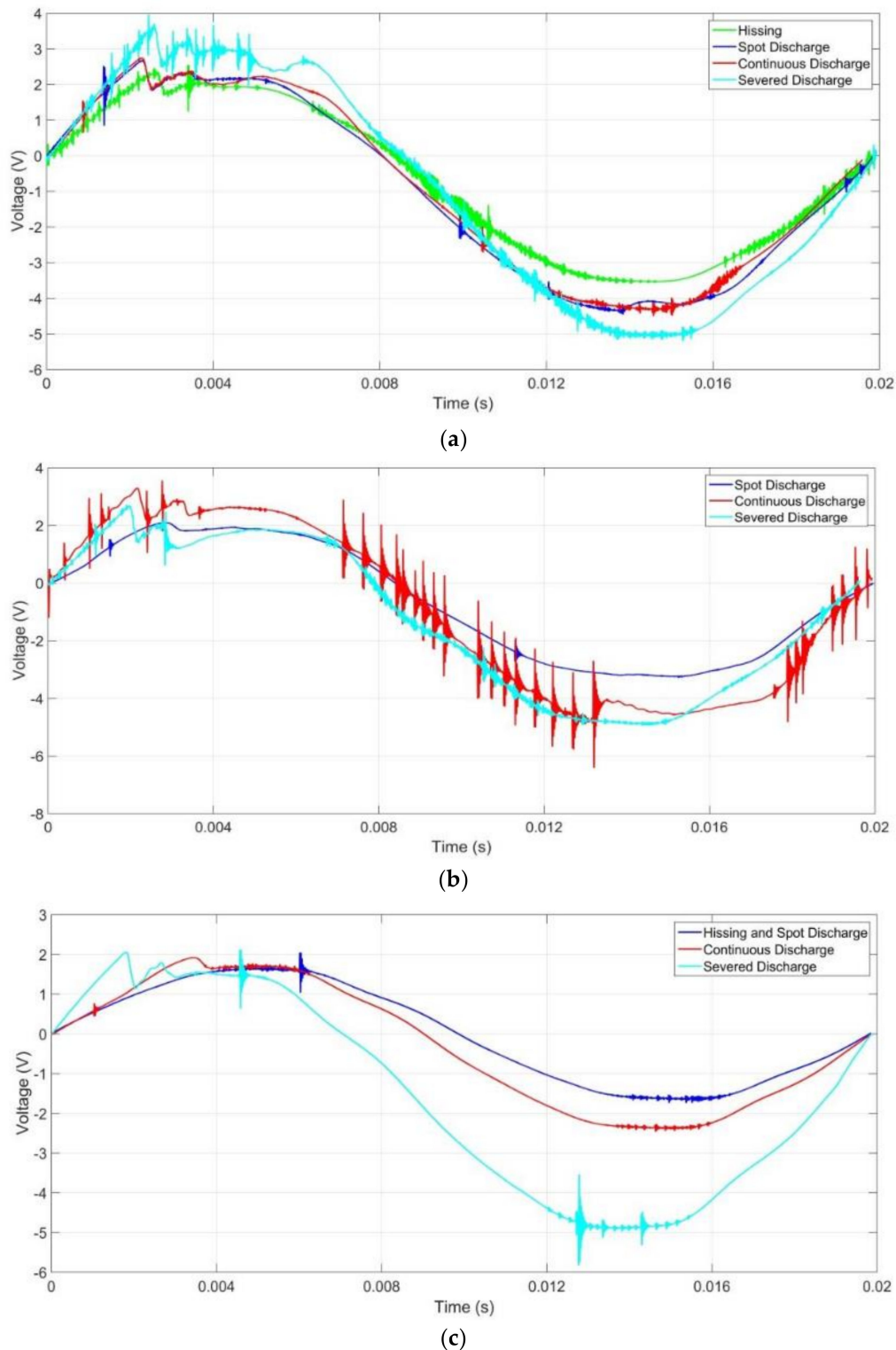


**Figure 12.** UV signals for insulator samples under wet conditions with light contamination level: (a) Group A; (b) Group B; (c) Group C.

Tables 12–14 show the injected voltages and average peak-to-peak voltage of the UV signal waveforms for the contaminated insulator samples under wet conditions for light, medium, and heavy contamination levels, respectively. It can be seen from the results that due to very low resistances of the Group B and C insulator samples’ surfaces, the injected voltages applied to produce a discharge were much lower than clean contaminated insulators (both dry and wet conditions). Furthermore, hissing discharge was not observed, as the electrical stress experienced on the insulator samples led straight to spot discharges, as in the case of light and medium contamination. While for heavy contamination, the electrical stress applied led to continuous discharges.

**Table 12.** Injected voltage and average peak-to-peak voltages of the UV signals for wet insulators conditions with light contamination level.

Sample Voltages Discharge Intensity Level	Group A		Group B		Group C	
	Range Injected Voltage, $V_i$ (kV)	Average Peak-to-Peak Voltage, $V_{p-p}$ (V)	Range Injected Voltage, $V_i$ (kV)	Average Peak-to-Peak Voltage, $V_{p-p}$ (V)	Range Injected Voltage, $V_i$ (kV)	Average Peak-to-Peak Voltage, $V_{p-p}$ (V)
Hissing	4–19	5.8	-	-	-	-
Spot Discharge	10–26	7.1	6–21	5.3	3–8	3.3
Continuous Discharge	26–31	7.2	11–28	8.1	10–18	4.3
Severe	24–41	8.7	20–31	7.6	19–34	6.9

**Table 13.** Injected voltage and average peak-to-peak voltages of the UV signals for wet insulators conditions with medium contamination level.

Sample Voltages Discharge Intensity Level	Group A		Group B		Group C	
	Range Injected Voltage, $V_i$ (kV)	Average Peak-to-Peak Voltage, $V_{p-p}$ (V)	Range Injected Voltage, $V_i$ (kV)	Average Peak-to-Peak Voltage, $V_{p-p}$ (V)	Range Injected Voltage, $V_i$ (kV)	Average Peak-to-Peak Voltage, $V_{p-p}$ (V)
Hissing	4–19	5.8	-	-	-	-
Discharge at pin	10–26	7.1	6–21	5.3	3–8	3.3
Discharge at cap	26–31	7.2	11–28	8.1	10–18	4.3
Severe	24–41	8.7	20–31	7.6	19–34	6.9

**Table 14.** Injected voltage and average peak-to-peak voltages of the UV signals for wet insulators conditions with heavy contamination level.

Sample Voltages Discharge Intensity Level	Group A		Group B		Group C	
	Range Injected Voltage, $V_i$ (kV)	Average Peak-to-Peak Voltage, $V_{p-p}$ (V)	Range Injected Voltage, $V_i$ (kV)	Average Peak-to-Peak Voltage, $V_{p-p}$ (V)	Range Injected Voltage, $V_i$ (kV)	Average Peak-to-Peak Voltage, $V_{p-p}$ (V)
Hissing	-	-	-	-	-	-
Discharge at pin	3–18	9.8	4–17	3.1	-	-
Discharge at cap	9–20	8.5	9–24	4.7	9–14	2.7
Severe	20–31	12.2	17–29	7.2	17–27	6.9

It is also worth noting that as the discharges became severe, the amplitude of the voltage waveforms were becoming smaller especially for Group B and C insulators, as shown in Figure 13. This is due to the fact that these groups of insulator samples were aged; their surface resistances had further been reduced by contamination, therefore the intense arcing activities on their surface created ohmic heating which dried up the insulator, and thus created higher resistance paths and spots on the surface of the insulators.

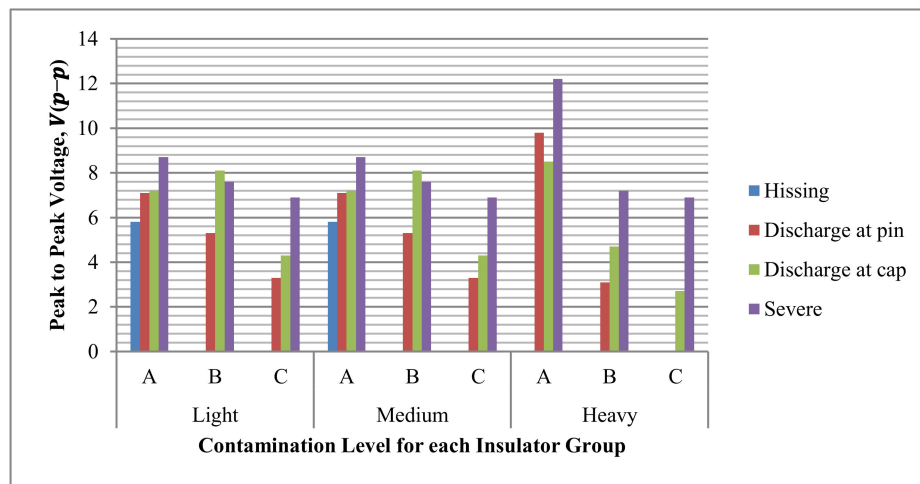


**Figure 13.** Average peak-to-peak voltage for each contamination level and insulator group for wet condition.

### 3.3. Analysis of UV Signals Frequency Components

#### 3.3.1. Total Harmonic Distortion

From Section 3.2, a correlation between the severity of the discharge and signal distortion was observed. In view of this, the FFT analysis to determine the THD values of the UV signals for all conditions were computed and analysed in this section.

#### Dry Conditions

Figure 14 presents the THD of the insulator samples UV signals under dry conditions.

From Figure 14, with respect to contamination levels, it can be seen that there is a general trend in the THD values of the insulator samples as their discharge intensity increased. At hissing discharge level, the signal distortion was normally low. As the discharge intensities increased, the disturbances increased which gave rise to harmonics, thus leading to the increase in the THD levels of the UV signal.

However, with respect to the degree of insulator ageing, a strong correlation did not seem to exist for all cases. In some cases, the THD of the most severely corroded (Group C) insulators were lower than the mildly corroded insulator (Group B). This may be attributed to the surface condition. Under dry surface condition, LC and surface resistances of insulators tend to be low with very little difference with respect to their contamination levels. However, when the contamination becomes moist, then a marked difference in the LC or surface resistance is noticed due to the conductive nature of the contamination level.

Table 15 shows the average THD values of the insulator samples with respect to discharge intensity levels irrespective of contamination levels. From the table, an increasing pattern in the THD values in relation to discharge intensity levels can be seen clearly.

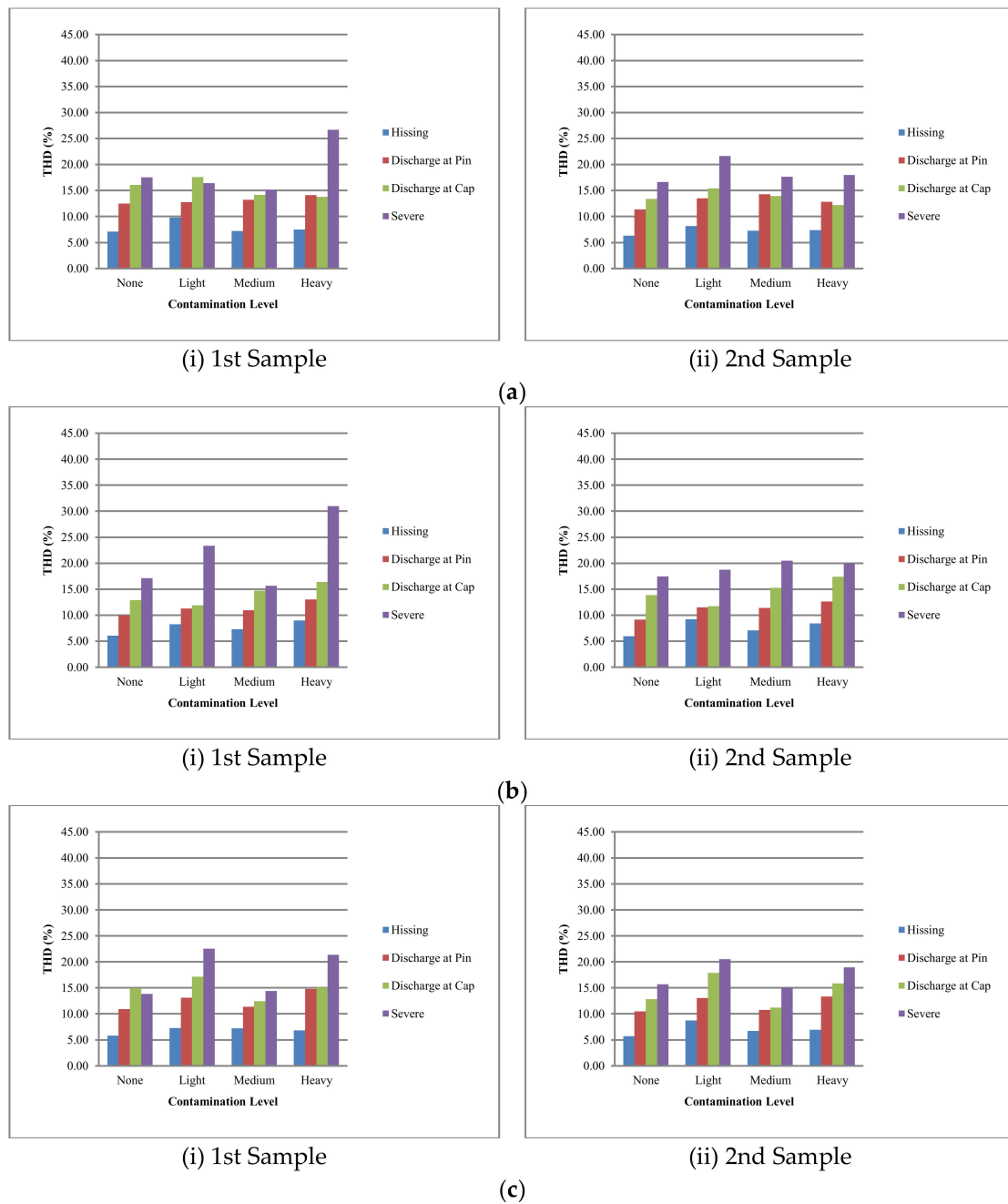


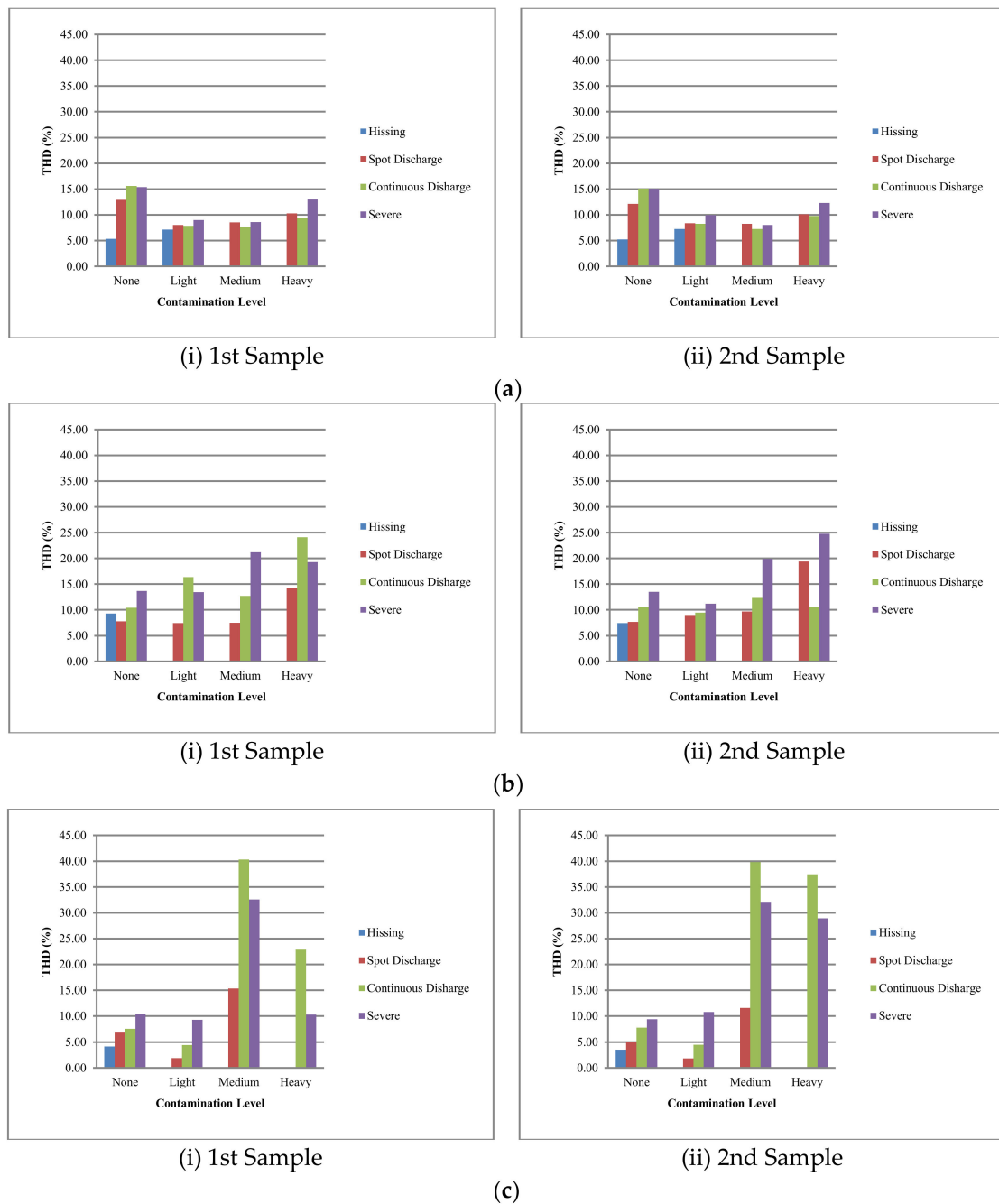
Figure 14. THD for dry insulator condition for samples of: (a) Group A; (b) Group B; (c) Group C.

Table 15. Average THD (%) for dry condition.

Discharge Intensity Level	Groups A		B		C	
	Sample 1	Sample 2	Sample 1	Sample 2	Sample 1	Sample 2
Hissing	7.90	7.29	7.65	7.65	6.79	7.02
Discharge at Pin	13.13	12.98	11.30	11.17	12.56	11.90
Discharge at Cap	15.39	13.73	13.98	14.57	14.90	14.46
Severe	18.96	18.48	21.77	19.16	18.03	17.56

Wet Conditions

Figure 15 presents the THD of the insulator samples UV signals under wet conditions



**Figure 15.** THD (%) for wet insulator condition for samples of: (a) Group A; (b) Group B; (c) Group C insulators.

From Figure 15, it can be clearly be seen that a strong correlation exists between the THD and both contamination level and degree of ageing. The THD values of the insulator samples were increasing as the discharge intensity levels increased. Furthermore, Group C (severely corroded) insulator samples possessed the highest THD values followed by Group B (mildly corroded). The corrosion on their surfaces provided more conduction in addition to the moist contamination. The THD of Group C insulators reached as high as 40%, while Group A insulators were less than 15% for all cases of contamination levels. In contrast, under dry contamination, most of the THD values were below 25%. This indicates the danger moisture contamination poses to insulators in service towards flashover incidence.

Table 16 shows the average THD values of the insulator samples under wet conditions with respect to discharge intensity levels irrespective of contamination levels. Similar to dry condition, an increasing pattern can also be seen in the THD values in relation to discharge intensity levels.

Table 16. Average THD (%) for wet condition.

Discharge Intensity Level	A		B		C	
	Sample 1	Sample 2	Sample 1	Sample 2	Sample 1	Sample 2
Hissing	3.11	3.11	2.32	1.86	1.03	0.87
Discharge at Pin	9.94	9.72	9.23	11.45	6.06	4.2
Discharge at Cap	10.12	10.08	15.91	10.72	18.78	22.38
Severe	11.48	11.32	16.89	17.33	15.62	20.32

### 3.3.2. Fundamental Frequency Component

In this section, results on the fundamental frequency components of the UV signals are presented, analysed, and discussed. The data was analyzed using the FFT method. Prior to using the FFT to find the harmonics component of the UV signals, the signals detected from the sensors were filtered using a simple Butterworth filter design in MATLAB tools. The filter was designed to filter out noise signals from the UV signals sensor.

#### Dry Conditions

Figure 16 shows the fundamental frequency component for dry conditions produced by the UV sensors signals

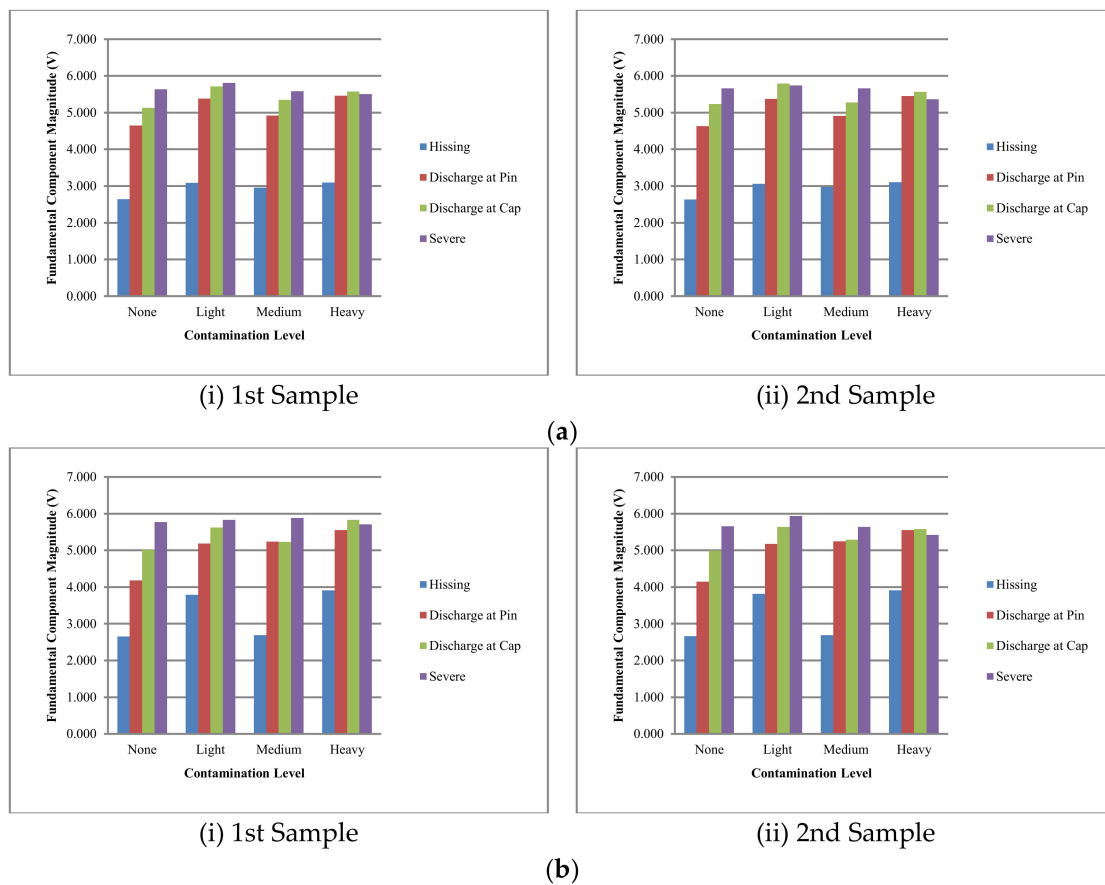
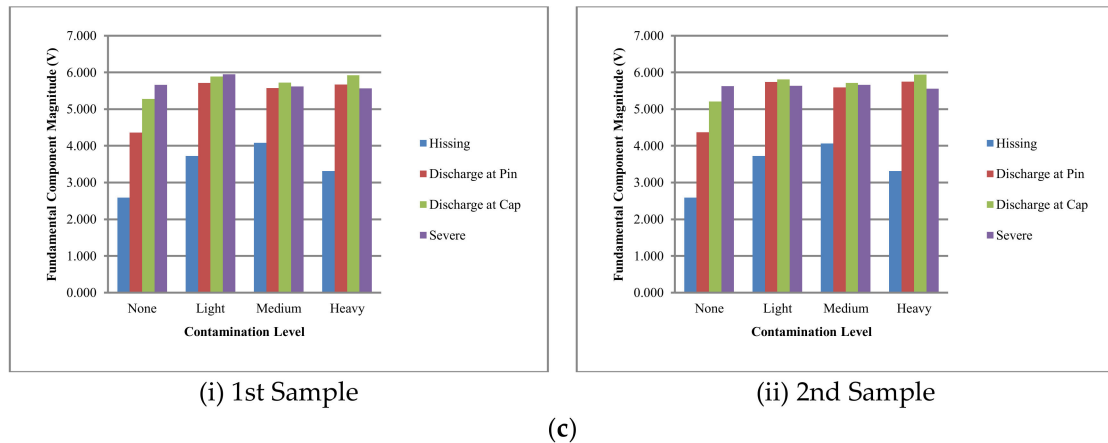


Figure 16. Cont.



**Figure 16.** Fundamental frequency components for dry condition for samples: (a) Group A; (b) Group B; (c) Group C insulators.

From Figure 16, it can be seen that a correlation exists between the fundamental frequencies of the UV signals and discharge intensity levels. However, with respect to degree of ageing, it can be seen that the entire insulator sample groups almost have the same voltage magnitude of fundamental frequency component. As earlier mentioned, under dry surface condition, irrespective of contamination level or ageing, insulators tend to have almost the same surface resistances or LC values. This explains the reason why the fundamental frequencies were almost of the same magnitude.

Wet Conditions

Figure 17 shows the fundamental frequency component of the UV signals under wet conditions. The discharge intensities of the insulator samples under wet conditions was higher than under dry condition. It can be seen that, similar to dry surface conditions, the fundamental frequency magnitudes were increasing with increasing discharge intensities. However, with respect to degree of ageing, the fundamental frequencies magnitudes were decreasing as the insulator surface degradation increased. This decrease in the magnitudes of the fundamental frequencies can be attributed to the intense discharges on the surface of the insulator samples. Moisture and the severe surface degradation resulted in intense discharges that lead to dry band on the surface of the insulator due to ohmic heating. This resulted in the increase of surface resistance, and thus lower arc/discharge current and consequently voltage.

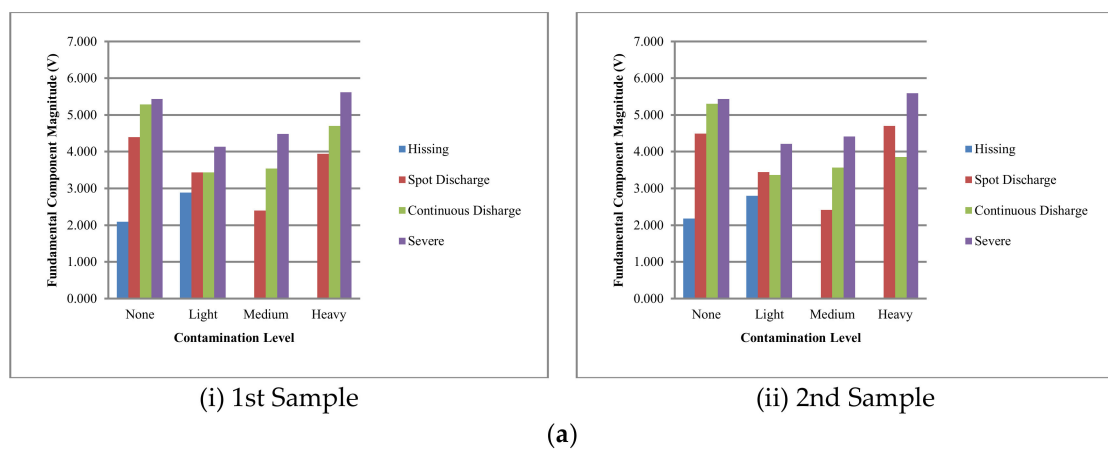


**Figure 17.** Cont.

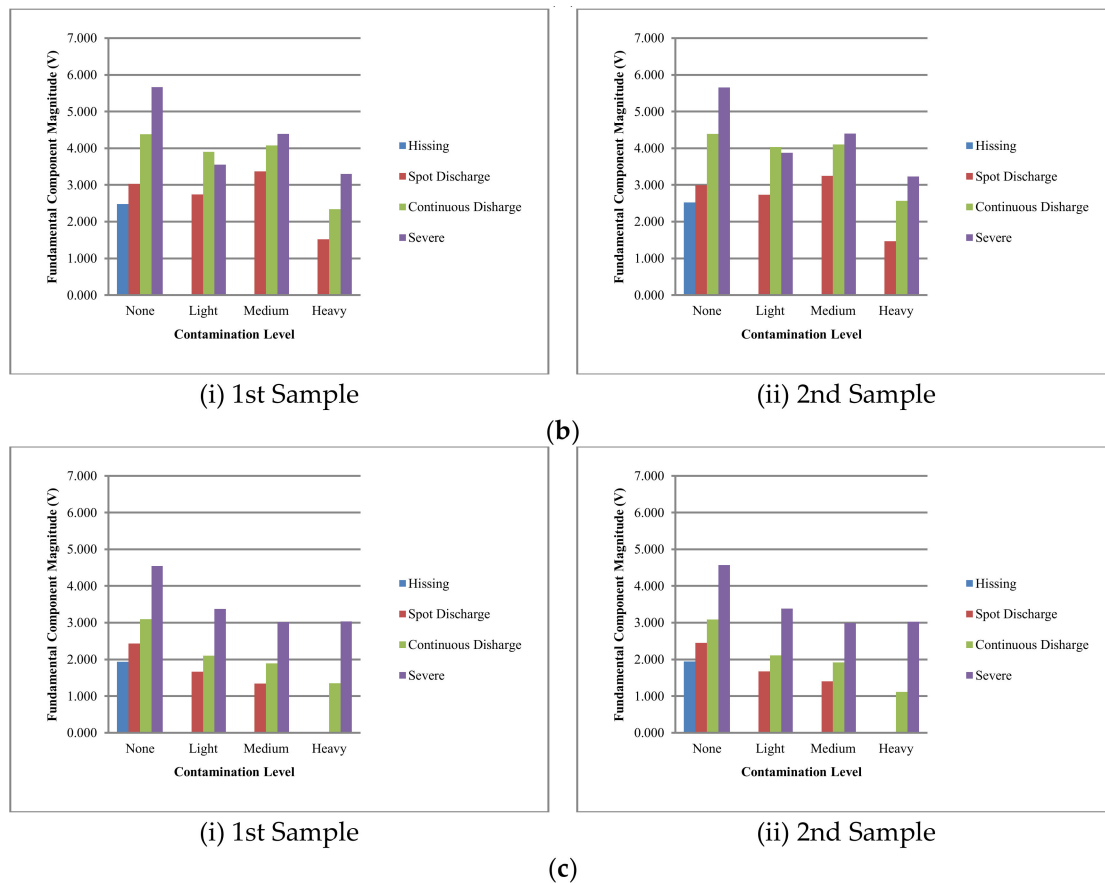


**Figure 17.** Fundamental frequency components for wet condition for samples: (a) Group A; (b) Group B; (c) Group C insulators.

### 3.3.3. Contamination Flashover Prediction Using ANN

The UV signals detected during discharge activities have shown to exhibit some patterns with respect to insulator contamination levels and degree of ageing. The THD and fundamental frequency components of the UV signals demonstrated correlations with the discharge intensity levels of the insulator samples based on the results discussed in Sections 3.2 and 3.3. It can be suggested that the UV pulses can be used to characterize and recognize discharge intensity levels based on the THD and fundamental component of the UV signals detected. Therefore based on these findings, ANN was employed for pattern recognition purpose to predict the occurrence of flashover on transmission lines.

### 3.4. Artificial Neural Network (ANN) Simulation Results

Table 17 shows the output of the ANN during testing after the training phase. It can be seen from the simulation results, that out of the 30 data sets used to test the ANN, only four data sets were incorrectly predicted (data of samples no. 5, 11, 26, and 27). It could be said that the ANN designed have an accuracy of 87% performance level. The performance of ANN was determined using Equation (2).

$$\text{Performance}(\%) = \frac{\text{Number of correctly recognized intensity level}}{\text{Total number of sample tested}} \times 100\% \quad (2)$$

**Table 17.** Artificial neural network simulation results.

Samples	Flashover Indication	Neural Network Output		
		1	2	3
Sample 1	Warning	0.84	0.00	0.05
Sample 2	Warning	0.98	0.00	0.05
Sample 3	Warning	0.93	0.00	0.10
Sample 4	Warning	0.94	0.00	0.01
Sample 5	Warning	0.68	0.00	0.11
Sample 6	Warning	1.00	0.00	0.00
Sample 7	Warning	0.94	0.00	0.06
Sample 8	Warning	0.96	0.00	0.06
Sample 9	Warning	0.80	0.00	0.06
Sample 10	Warning	1.00	0.00	0.00
Sample 11	Danger (dry)	0.00	0.22	0.77
Sample 12	Danger (dry)	0.00	1.00	0.00
Sample 13	Danger (dry)	0.00	1.00	0.00
Sample 14	Danger (dry)	0.00	1.00	0.00
Sample 15	Danger (dry)	0.00	0.99	0.02
Sample 16	Danger (dry)	0.00	0.89	0.34
Sample 17	Danger (dry)	0.00	1.00	0.00
Sample 18	Danger (dry)	0.00	1.00	0.03
Sample 19	Danger (dry)	0.00	1.00	0.00
Sample 20	Danger (dry)	0.00	1.00	0.00
Sample 21	Danger (wet)	0.062	0.01	0.87
Sample 22	Danger (wet)	0.08	0.00	0.95
Sample 23	Danger (wet)	0.00	0.00	1.00
Sample 24	Danger (wet)	0.00	0.00	1.00
Sample 25	Danger (wet)	0.00	0.00	1.00
Sample 26	Danger (wet)	0.85	0.00	0.14
Sample 27	Danger (wet)	0.88	0.00	0.19
Sample 28	Danger (wet)	0.00	0.00	1.00
Sample 29	Danger (wet)	0.00	0.00	1.00
Sample 30	Danger (wet)	0.01	0.00	1.00

#### 4. Conclusions

This research work presents a study on insulator surfaces discharges using the UV pulse method. The UV radiations emitted by varying discharge intensities were studied under various contamination levels and degree of ageing. The main findings from this work are as follows:

1. Insulator surface discharges under varying contamination levels and degradation levels from UV signals using the UV pulse voltage method were studied. The UV signal voltages and waveforms due to presence of surface discharges were analyzed.
2. Based on the experimental results under wet surface conditions, a strong correlation exists between the frequency components of the UV signals and discharge intensity levels under varying contamination levels and varying degree of ageing. As the contamination levels increased, the discharge intensity levels of the insulator samples increased resulting in the increase of the UV signal THD and fundamental frequency component.
3. Under dry surface conditions, similar correlations for wet surface conditions were observed, however, no correlation was observed between the frequency components of the UV signals and discharge intensity levels under varying degrees of ageing.
4. Fundamental frequency components and THD of the UV signal were successfully used to predict the imminence of flashover using ANN, yielding an 87% performance level.

Based on the above findings, the objectives of the research were successfully achieved.

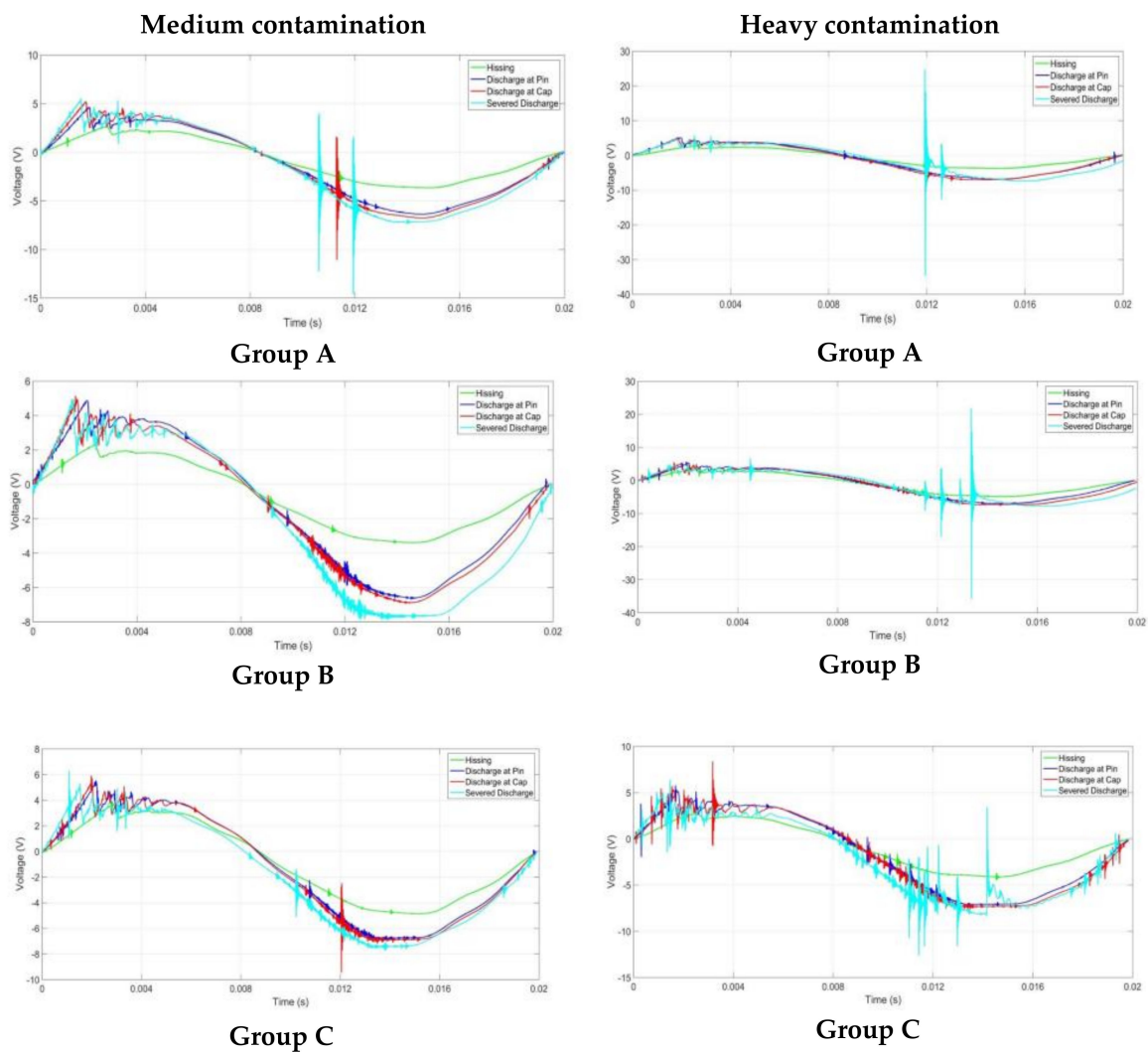
**Author Contributions:** S.M.I.S. conducted the experiments and analyzed the data; N.B. supervised the project co-analyzed the data, and reviewed the paper; N.A.A. co-supervised the project and reviewed the paper; N.N.A.R. drafted the paper; N.A.M. supervised the project, co-analyzed the data, reviewed the paper and provided final approval of the version to be published. M.N.A.R. reviewed the paper.

**Funding:** This research was supported by USM short term grant (304/pelect/6315032) and RUI (1001/PELECT/8014054); UTM Research University Grant vot no. 0H77.

**Conflicts of Interest:** The authors declare no conflict of interest.

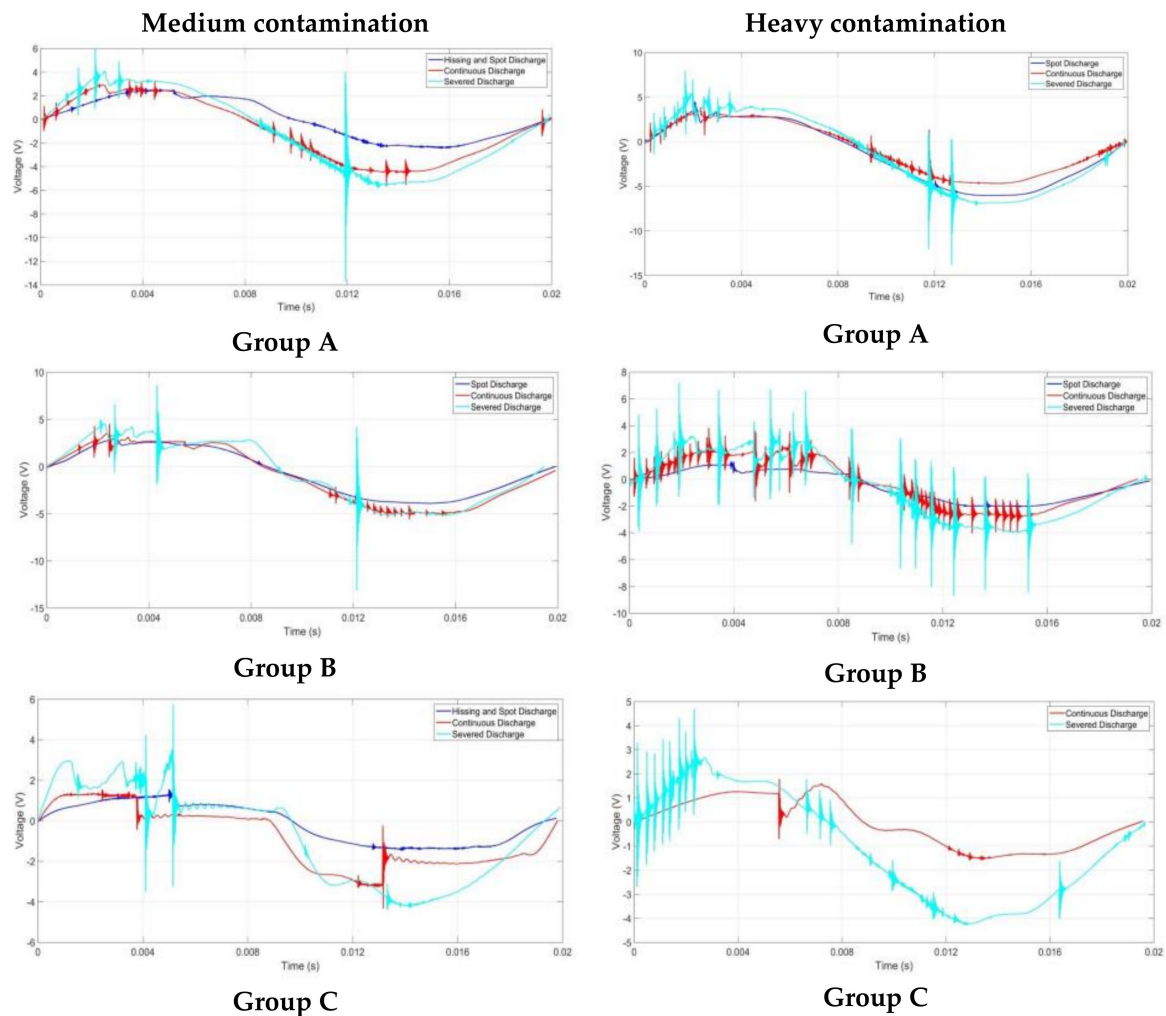
### Appendix A

Ultraviolet signals for insulator samples for each group under dry conditions for medium and heavy contamination levels.



### Appendix B

Ultraviolet signals for Group A insulator samples under wet conditions for medium and heavy contamination levels.



## References

1. Looms, J.S.T. *Insulators for High Voltages*; Peter Perengrinnus Ltd.: Exeter, UK, 1988.
2. Hussain, M.M.; Farokhi, S.; McMeekin, S.; Farzaneh, M. Mechanism of saline deposition and surface flashover on outdoor insulators near coastal areas part II: Impact of various environment stresses. *IEEE Trans. Dielectr. Electr. Insul.* **2017**, *24*, 1068–1076. [[CrossRef](#)]
3. Tian, Y.; Lewin, P.; Davies, A. Comparison of on-line partial discharge detection methods for HV cable joints. *IEEE Trans. Dielectr. Electr. Insul.* **2002**, *9*, 604–615. [[CrossRef](#)]
4. Markalous, S.M.; Tenbohlen, S.; Feser, K. Detection and location of partial discharges in power transformers using acoustic and electromagnetic signals. *IEEE Trans. Dielectr. Electr. Insul.* **2008**, *15*, 1576–1583. [[CrossRef](#)]
5. Blitshteyn, M.; Zabita, J. Infrared thermography of negative DC and negatively enhanced AC point-to-plane corona discharge in air. *IEEE Trans. Ind. Appl.* **1988**, *24*, 745–748. [[CrossRef](#)]
6. Wang, S.; Lv, F.; Liu, Y. Estimation of discharge magnitude of composite insulator surface corona discharge based on ultraviolet imaging method. *IEEE Trans. Dielectr. Electr. Insul.* **2014**, *21*, 1697–1704. [[CrossRef](#)]
7. Zhao, W.; Zhang, X.; Jiang, J. Tip to plane Corona discharge spectroscopic analysis. *Spectrosc. Spectr. Anal.* **2003**, *23*, 955–957.
8. Lu, F.; Wang, S.; Li, H. Insulator pollution grade evaluation based on ultraviolet imaging and fuzzy logic inference. In Proceedings of the 2010 Asia-Pacific Power and Energy Engineering Conference (APPEEC), Chengdu, China, 28–31 March 2010; pp. 1–4.
9. Wang, S.; Lu, F.; Chen, L.; Li, H. Study of polymeric insulator external insulation based on UV imaging method. In Proceedings of the IEEE 9th International Conference on the Properties and Applications of Dielectric Materials (ICPADM 2009), Harbin, China, 19–23 July 2009; pp. 1043–1046.

10. Hu, B.; Ma, L.-X.; Yuan, S.-J.; Yang, B. New corona ultraviolet detection system and fault location method. In Proceedings of the 2012 China International Conference on Electricity Distribution (CICED), Shanghai, China, 10–14 September 2012; pp. 1–4.
11. Jin, L.; Zhang, D. Contamination grades recognition of ceramic insulators using fused features of infrared and ultraviolet images. *Energies* **2015**, *8*, 837–858. [[CrossRef](#)]
12. Ai, J.; Jin, L.; Zhang, Y.; Tian, Z.; Peng, C.; Duan, W. Detecting partial discharge of polluted insulators based on ultraviolet imaging. In Proceedings of the 2015 IEEE 11th International Conference on the Properties and Applications of Dielectric Materials (ICPADM), Sydney, Australia, 19–22 July 2015; pp. 456–459.
13. Zhao, W.; Liu, W.; Hu, Y.; An, Y.; Li, Y. Extraction method of insulator discharge area in ultraviolet image and its application. In Proceedings of the 2017 4th International Conference on Systems and Informatics (ICSAI), Hangzhou, China, 11–13 November 2017; pp. 857–961.
14. Hamamatsu. Flame Sensor UVTRON R2868. Available online: [https://www.hamamatsu.com/resources/pdf/etd/R2868\\_TPT1008E.pdf](https://www.hamamatsu.com/resources/pdf/etd/R2868_TPT1008E.pdf) (accessed on 15 September 2015).
15. IEC60507. *Artificial Pollution Tests on High-Voltage Insulators to Be Used on AC Systems*; International Electrotechnical Commission: Geneva, Switzerland, 1991.
16. IEC60815. *Guide for the Selection of Insulators in Respect of Polluted Conditions*; International Electrotechnical Commission: Geneva, Switzerland, 1986.
17. Jayalakshimi, T.; Santhakumaran, A. Statistical Normalization and Back Propagation for Classification. *Int. J. Comput. Theory Eng.* **2011**, *3*, 1793–8201.
18. IEEE Standard 957-2005. *IEEE Guide for Cleaning Insulators*; IEEE Standards: Piscataway, NJ, USA, 2005.



© 2019 by the authors. Licensee MDPI, Basel, Switzerland. This article is an open access article distributed under the terms and conditions of the Creative Commons Attribution (CC BY) license (<http://creativecommons.org/licenses/by/4.0/>).